The Plant Cell, Vol. 25: 762–776, February 2013, www.plantcell.org

The *Arabidopsis* Elongator Complex Subunit2 Epigenetically Regulates Plant Immune Responses[W][OA]

Yongsheng Wang,[a] Chuanfu An,[a] Xudong Zhang,[a] Jiqiang Yao,[b] Yanping Zhang,[b] Yijun Sun,[b] Fahong Yu,[b] David Moraga Amador,[b] and Zhonglin Mou[a,1]

[a] Department of Microbiology and Cell Science, University of Florida, Gainesville, Florida 32611
[b] Interdisciplinary Center for Biotechnology Research, University of Florida, Gainesville, Florida 32610

The *Arabidopsis thaliana* Elongator complex subunit2 (ELP2) genetically interacts with NONEXPRESSOR OF PATHOGENESIS-RELATED GENES1 (NPR1), a key transcription coactivator of plant immunity, and regulates the induction kinetics of defense genes. However, the mechanistic relationship between ELP2 and NPR1 and how ELP2 regulates the kinetics of defense gene induction are unclear. Here, we demonstrate that ELP2 is an epigenetic regulator required for pathogen-induced rapid transcriptome reprogramming. We show that ELP2 functions in a transcriptional feed-forward loop regulating both *NPR1* and its target genes. An *elp2* mutation increases the total methylcytosine number, reduces the average methylation levels of methylcytosines, and alters (increases or decreases) methylation levels of specific methylcytosines. Interestingly, infection of plants with the avirulent bacterial pathogen *Pseudomonas syringae* pv *tomato* DC3000/*avrRpt2* induces biphasic changes in DNA methylation levels of *NPR1* and *PHYTOALEXIN DEFICIENT4* (*PAD4*), which encodes another key regulator of plant immunity. These dynamic changes are blocked by the *elp2* mutation, which is correlated with delayed induction of *NPR1* and *PAD4*. The *elp2* mutation also reduces basal histone acetylation levels in the coding regions of several defense genes. Together, our data demonstrate a new role for Elongator in somatic DNA demethylation/methylation and suggest a function for Elongator-mediated chromatin regulation in pathogen-induced transcriptome reprogramming.

INTRODUCTION

Immune responses are essential for both plants and animals to defend against microbial pathogens. Unlike animals, plants do not have any mobile cells specialized for defense but instead rely on individual cells to recognize pathogens and activate immune responses. In response to pathogen attack, plant cells reprogram their transcriptional profiles to mount a defense at the expense of normal cellular functions. The strength of the defense correlates with the kinetics and magnitude of the transcriptional changes. Suppressing or delaying pathogen-induced transcription by pathogenic effectors or mutations in the defense machinery compromises resistance (Tao et al., 2003; Jones and Dangl, 2006). Thus, it is crucial for plant cells to rapidly and efficiently reprogram transcription to fight infection.

In eukaryotic cells, RNA Polymerase II catalyzes the transcription of protein-encoding genes. A multitasking protein complex named Elongator was first identified as an interactor of hyperphosphorylated (elongating) RNA Polymerase II in yeast (Otero et al., 1999) and was later purified from human and *Arabidopsis thaliana* cells (Hawkes et al., 2002; Kim et al., 2002; Nelissen et al., 2010). Elongator consists of six subunits (Elongator complex subunit1 [ELP1]/ELONGATA2 [ELO2]/ABSCISIC ACID-OVERLY SENSITIVE1, ELP2, ELP3/ELO3, ELP4/ELO1, ELP5, and ELP6) that act together as a functional unit, with ELP1 and ELP2 serving as scaffolds for complex assembly, ELP3 being the catalytic subunit, and ELP4-6 forming an accessory complex. Loss of any Elongator subunit compromises its integrity, rendering the complex inactive (Versées et al., 2010). Elongator has been shown to function in several distinct cellular processes, including histone modification, tRNA modification, exocytosis, α-tubulin acetylation, and zygotic paternal genome demethylation (Hawkes et al., 2002; Huang et al., 2005; Rahl et al., 2005; Creppe et al., 2009; Okada et al., 2010). Mutations in yeast Elongator subunits lead to resistance to the zymocin γ-toxin subunit, defects in transcriptional silencing, and sensitivity to salt, caffeine, temperature, and DNA damaging agents (Otero et al., 1999; Jablonowski et al., 2001; Krogan and Greenblatt, 2001). In humans, Elongator deficiency causes familial dysautonomia, an autosomal recessive disease characterized by abnormally low numbers of neurons in the autonomic and sensory nervous systems (Anderson et al., 2001; Slaugenhaupt et al., 2001). In *Arabidopsis*, mutations of Elongator subunits result in pleiotropic effects, including hypersensitivity to abscisic acid, resistance to oxidative stress, severely aberrant auxin phenotypes, disease susceptibility, and altered cell cycle progression (Nelissen et al., 2005, 2010; Chen et al., 2006; Zhou et al., 2009; DeFraia et al., 2010; Xu et al., 2012).

The Elongator catalytic subunit ELP3 harbors a C-terminal histone acetyltranferase (HAT) domain and an N-terminal Cys-rich motif that resembles an iron-sulfur radical *S*-adenosylmethionine (SAM) domain (Chinenov, 2002; Winkler et al., 2002). ELP3 has intrinsic HAT activity and is capable of acetylating all four histones, whereas the six-subunit holo-Elongator predominantly acetylates

[1] Address correspondence to zhlmou@ufl.edu.
The author responsible for distribution of materials integral to the findings presented in this article in accordance with the policy described in the Instructions for Authors (www.plantcell.org) is: Zhonglin Mou (zhlmou@ufl.edu).
[W] Online version contains Web-only data.
[OA] Open Access articles can be viewed online without a subscription.
www.plantcell.org/cgi/doi/10.1105/tpc.113.109116

Lys-14 of histone H3 and Lys-8 of histone H4 (Wittschieben et al., 1999; Winkler et al., 2002). Subsequently, the levels of acetylated histones H3 and H4 are reduced in yeast, human, and *Arabidopsis elp* mutants (Winkler et al., 2002; Close et al., 2006; Nelissen et al., 2010). Elongator may also have another catalytic function suggested by the fact that the archaea *Methanocaldococcus jannaschii* ELP3 binds and cleaves SAM (Paraskevopoulou et al., 2006). Indeed, a recent study indicated that the radical SAM domain of mouse ELP3, but not the HAT domain, is required for Elongator's function in zygotic paternal genome demethylation (Okada et al., 2010), suggesting that mouse ELP3 may be a radical SAM protein catalyzing active DNA demethylation in zygotes. However, it is unknown whether Elongator functions in DNA demethylation in nondividing somatic cells and whether this activity is evolutionarily conserved in plants.

Previous characterization of loss-of-function mutants of *Arabidopsis* ELP2 revealed that *elp2* genetically interacts with a mutation in *NONEXPRESSOR OF PATHOGENESIS-RELATED GENES1* (*NPR1*)/*NONINDUCIBLE IMMUNITY1*/*SALICYLIC ACID INSENSITIVE1* (*SAI1*), which encodes a key transcription coactivator regulating plant immunity (Cao et al., 1997; Ryals et al., 1997; Shah et al., 1997; DeFraia et al., 2010). Whereas NPR1 mostly affects the scale of defense gene expression, ELP2 regulates the kinetics of defense gene induction. Simultaneous removal of NPR1 and ELP2 completely compromises the resistance mediated by two different plant resistance (R) proteins, demonstrating the distinction between ELP2 and NPR1. At the transcriptional level, ELP2 regulates several NPR1 target genes, suggesting that ELP2 and NPR1 may have some overlapping functions. However, the mechanistic relationship between ELP2 and NPR1 in pathogen-induced transcriptional changes and how ELP2 regulates the kinetics of defense gene induction remain unclear.

Here, we performed in-depth characterization of the *elp2* mutant using microarrays, chromatin immunoprecipitation, and genome-wide or locus-specific bisulfite sequencing. Our results show that ELP2 regulates the kinetics of pathogen-induced transcriptome reprogramming, maintains histone acetylation levels in several defense genes, modulates the genomic DNA methylation landscape, and influences pathogen-induced dynamic DNA methylation changes. Thus, Elongator plays an evolutionarily conserved role in DNA demethylation/methylation in plants and likely functions as an epigenetic regulator of plant immune responses.

RESULTS

The *elp2* Mutation Exhibits a Broader and Stronger Impact Than *npr1* on Pathogen-Induced Transcriptome Changes

In order to identify and compare ELP2 target genes with those of NPR1 at the genome level, we performed a microarray experiment to monitor the avirulent bacterial pathogen *Pseudomonas syringae* pv *tomato* (*Pst*) DC3000/*avrRpt2*-induced transcriptome changes in *elp2*, *npr1*, and the wild type (National Center for Biotechnology Information [NCBI] Gene Expression Omnibus series number GSE38986). Triplicate experiments were performed independently, and the data were analyzed to identify genes that were differentially expressed between *elp2* or *npr1* and the wild type. We used P values to identify differentially expressed candidate genes between *elp2* and the wild type and then performed real-time quantitative PCR (qPCR) to verify the identified genes. Eight thus selected defense genes were all confirmed to be differentially expressed between *elp2* and the wild type (Figure 1E); therefore, the P values computed for microarray analysis were not corrected for multiple testing. Genes that showed a twofold or larger difference in their expression levels with a low P value ($\leq$0.05) were chosen for further analysis. Considerably more genes were differentially expressed between *elp2* and the wild type than between *npr1* and the wild type (Figure 1A). A total of 568, 2336, 2951, and 1218 genes were differentially expressed between *elp2* and the wild type at 0, 4, 8, and 12 h after inoculation (hpi), respectively, whereas only 69, 558, 547, and 525 genes were differentially expressed between *npr1* and the wild type. These results suggest that the *elp2* mutation has a broader impact than *npr1* on *Pst* DC3000/*avrRpt2*-induced transcriptome changes. Thus, ELP2 is a more general regulator of transcription than NPR1 in *Pst* DC3000/*avrRpt2*-induced immune response.

To identity the degree of functional overlap between ELP2 and NPR1, we compared the differentially expressed genes in *elp2* and *npr1*. Surprisingly, we found that a large number of genes influenced by NPR1 were also under the regulation of ELP2 (Figure 1B; see Supplemental Figure 1A online). ELP2 and NPR1, as positive regulators of defense genes, exhibited the most dramatic overlapping functions at 4 hpi when ELP2 was required for the full expression of ~83.8% of the genes that were positively regulated by NPR1 (Figure 1B). These results indicate that ELP2 and NPR1 have significantly overlapping functions in plant immune responses.

To test whether ELP2 or/and NPR1 regulate the kinetics of pathogen-induced transcriptome changes, we queried the microarray data and identified genes that showed a twofold or higher induction or suppression with a low P value ($\leq$0.05) in *elp2*, *npr1*, and the wild type. We found that all three genotypes exhibited dramatic transcriptional reprogramming upon *Pst* DC3000/*avrRpt2* infection (Figure 1C). Interestingly, although both *elp2* and *npr1* significantly shifted their transcriptome profiles (Figure 1D; see Supplemental Figure 1B online), a dramatic effect on the kinetics of *Pst* DC3000/*avrRpt2*-induced transcriptome changes was seen only in *elp2* (Figure 1C). While the numbers of genes up- or downregulated in *npr1* and the wild type were highest at 8 hpi, in *elp2*, they were higher at 12 hpi. At 8 hpi, 3900 and 4461 genes in *npr1*, and 4242 and 4592 genes in the wild type were up- and downregulated, respectively, whereas only 2782 and 2796 genes in *elp2* were up- and downregulated, respectively. Even at 12 hpi, the numbers of genes up- or downregulated in *elp2* were still smaller than those in *npr1* and the wild type (Figure 1C). Therefore, the *elp2* genome responded more slowly to *Pst* DC3000/*avrRpt2* infection than those of *npr1* and the wild type, suggesting that the *elp2* mutation has a larger impact than *npr1* on pathogen-induced transcriptional reprogramming.

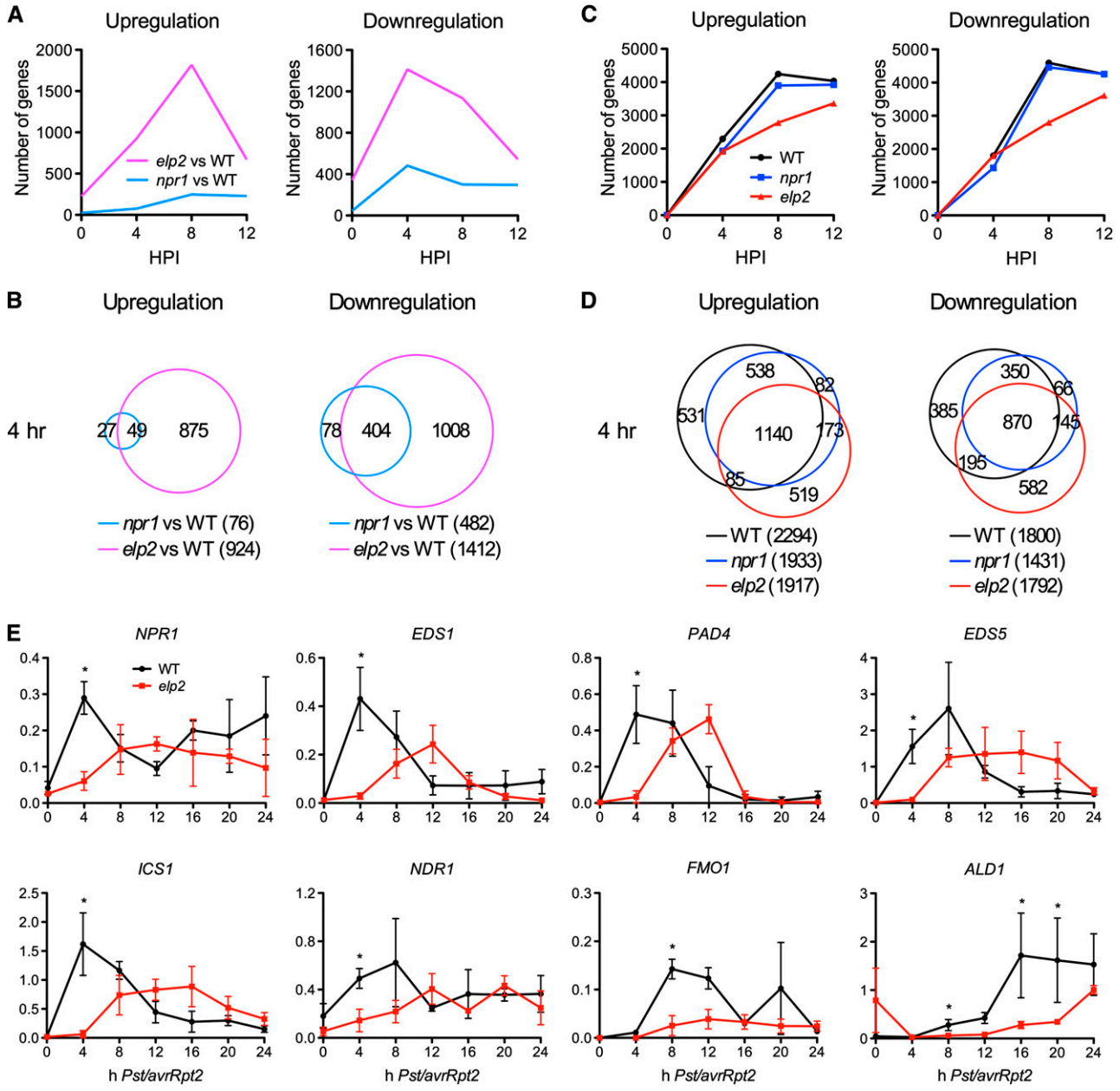

Figure 1. Pathogen-Induced Transcriptome Changes in *elp2*.

(A) Dynamic changes in the numbers of genes that are differentially expressed between *elp2* and the wild type (WT) and between *npr1* and the wild type after *Pst* DC3000/*avrRpt2* infection.

(B) Overlaps between the genes that are differentially expressed at 4 hpi between *elp2* and the wild type and those between *npr1* and the wild type.

(C) Dynamic changes in the numbers of genes that are up- or downregulated in the wild type, *npr1*, and *elp2* after *Pst* DC3000/*avrRpt2* infection.

(D) Overlaps among the genes that are up- or downregulated at 4 hpi in the wild type, *npr1*, and *elp2*.

(E) Expression of eight major defense genes in *Pst* DC3000/*avrRpt2*-infected wild-type and *elp2* plants. The *y* axes indicate relative expression levels monitored by qPCR (results in **[A]** to **[D]** were from microarray analysis). Expression levels were normalized against *UBQ5*. The *x* axes indicate hours after *Pst* DC3000/*avrRpt2* infection. Data represent the mean of three independent samples with SD. An asterisk indicates a significant difference between the wild type and *elp2* ($P < 0.05$, *t* test).

ELP2 Regulates *NPR1* and Its Target Genes

As a more general regulator of transcription, ELP2 might regulate pathogen-induced transcriptome changes through major defense genes, such as *NPR1* (Cao et al., 1997). To test this hypothesis, we analyzed the genes that were differentially expressed between *elp2* and the wild type. Interestingly, the induction of *NPR1* and many of the well-characterized major defense genes, such as *ENHANCED DISEASE SUSCEPTIBILITY1* (*EDS1*), *PHYTOALEXIN DEFICIENT4* (*PAD4*), *EDS5/SA INDUCTION DEFICIENT1*, *ISOCHORISMATE SYNTHASE1* (*ICS1*)/*SID2*/*EDS16*, *NON-RACE-SPECIFIC DISEASE RESISTANCE1* (*NDR1*), *AGD2-LIKE DEFENSE RESPONSE PROTEIN1* (*ALD1*), and *FLAVIN-DEPENDENT MONOOXYGENASE1* (*FMO1*), was either delayed or decreased in *elp2* compared with the wild type after *Pst* DC3000/*avrRpt2* infection (Table 1) (Century et al., 1997; Falk et al., 1999; Jirage et al., 1999; Wildermuth et al., 2001; Nawrath et al., 2002; Song et al., 2004; Mishina and Zeier, 2006). To confirm the microarray results, we used real-time qPCR to monitor the induction of these genes in *elp2* after DC3000/*avrRpt2* infection. As shown in Figure 1E, induction of all eight genes was delayed and/or decreased in *elp2*, suggesting that ELP2 may function upstream of these major defense genes to regulate plant immune responses.

Since ELP2 regulates *NPR1* induction, we expected that ELP2 would also regulate the expression of NPR1 target genes. Indeed, expression of the majority of the NPR1 target genes, which were identified in a previous study (Wang et al., 2005), were reduced in *elp2* compared with the wild type at either one or more of the four time points after *Pst* DC3000/*avrRpt2* infection (Table 1), suggesting that ELP2 is a key regulator of NPR1-mediated transcription. To find out how ELP2 is involved in the NPR1 transcriptional cascade, we crossed the well-characterized *35S*:*NPR1-GFP* (for green fluorescent protein) transgene into *elp2* and tested whether overexpression of *NPR1-GFP* could rescue the induction pattern of NPR1 target genes (Kinkema et al., 2000). As shown in Figure 2A, overexpression of *NPR1-GFP* did not restore the expression pattern of eight out of the nine tested NPR1 target genes. Furthermore, the heightened basal resistance conferred by overexpression of *NPR1-GFP* was completely suppressed by the *elp2* mutation (Figure 2B) (Cao et al., 1998). These results suggest that ELP2 may also function independently of NPR1 to regulate the transcription of NPR1 target genes.

ELP2 Regulates Histone Acetylation Levels in Several Defense Genes

Elongator possesses HAT activity essential for maintaining normal histone acetylation levels in yeast, humans, and plants (Winkler et al., 2002; Close et al., 2006; Nelissen et al., 2010). To test whether ELP2 is required for maintaining normal (basal) histone acetylation levels in defense genes, we assessed the acetylation status of histone H3 in *NPR1*, *PR1*, *PR2*, *PR5*, *EDS1*, and *PAD4* using chromatin immunoprecipitation. After formaldehyde cross-linking and cell lysis of *elp2* and wild-type leaf tissues, histone-DNA complexes were immunoprecipitated using an antibody specific for histone H3 acetylated at Lys-9 and -14 (H3K9/14ac). Precipitated DNA was quantified using real-time qPCR to estimate the levels of histone H3K9/14ac. Interestingly, although the basal expression levels of *NPR1*, *PR1*, *PR2*, *PR5*, *EDS1*, and *PAD4* were comparable in *elp2* and the wild type (see Supplemental Figure 2 online), histone H3K9/14ac levels in the coding regions of these defense genes except *PR1* were significantly lower in *elp2* than in the wild type (Figure 3). Since histone acetylation is generally associated with transcriptional activation (Workman and Kingston, 1998), reduced basal histone acetylation levels may contribute to the delayed or/and decreased induction of defense genes in *elp2*.

ELP2 Modulates DNA Methylation in *Arabidopsis*

As Elongator plays a critical role in paternal genome demethylation in mouse zygotes (Okada et al., 2010), we asked whether Elongator modulates DNA methylation in *Arabidopsis*. To address this question, we first analyzed DNA methylation levels using bisulfite sequencing of several ELP2-regulated defense genes (see Supplemental Table 1 online). Consistent with the results reported previously (Lister et al., 2008), the cytosines in the sequenced regions of *NPR1* and *PAD4* were significantly methylated, while those in *PR1*, *PR2*, and *PR5* (except three cytosines in *PR2*) were not methylated (Figure 4; see Supplemental Figure 3 online). Methylation occurred at CG, CHG, and CHH sites in the *NPR1* promoter region (Figures 4A and 4B; see Supplemental Figure 3A online) but was largely restricted to CG dinucleotides in the *NPR1* and *PAD4* coding regions (Figures 4C and 4D). Interestingly, DNA methylation levels were generally higher in *elp2* than in the wild type except at the *NPR1* coding region, where DNA methylation levels were lower in *elp2*. In the *NPR1* promoter and the *PAD4* coding regions, methylation levels at several specific methylcytosines were significantly higher in *elp2* than in the wild type (Figures 4A, 4B, and 4D). These results indicate that ELP2 modulates basal DNA methylation levels in *NPR1* and *PAD4*, which could suggest that ELP2 regulates defense gene expression through DNA methylation.

To reveal broad effects of ELP2 on DNA methylation profiles, we generated genome-scale DNA methylation maps of *elp2* and the wild type using bisulfite deep sequencing (BS-Seq) (NCBI Short Read Archive accession number SRA055073). A total of 58,976,071 and 48,090,948 sequence reads were mapped in *elp2* and the wild type, respectively, of which 24,234,987 and 14,930,215 were unique (nonclonal); and a total of 3,850,501 cytosines were covered by at least 10 reads in both *elp2* and the wild type. Based on the reads aligned to the unmethylated chloroplast genome that was isolated and sequenced in conjunction with the nuclear genome, the average nonconversion rate of the bisulfite conversion was 0.28% and the average thymidine-to-cytosine sequencing error rate was 0.30% (see Supplemental Table 2 online). Using 0.58% (0.28% plus 0.30%) as a measure of the false methylcytosine discovery rate, a binomial probability distribution was used to calculate the minimum sequence depth at a cytosine position at which a methylcytosine could be called while maintaining a false positive rate below 5%. From the 3,850,501 cytosines, 2,204,921 were identified as methylcytosines in at least one genotype, which accounts for 5.12% of all genomic cytosine. These methylcytosines were used for further analysis.

Table 1. Defense Genes That Are Differentially Expressed between *elp2* and the Wild Type during *Pst* DC3000/*avrRpt2* Infection

		elp2/Wild Type								
		0 h		4 h		8 h		12 h		
AGI Locus	Gene name	Log_2 (FC)	P Value	Log_2 (FC)	P Value	Log_2 (FC)	P Value	Log_2 (FC)	P Value	AGI Description
Major defense genes										
At1g64280	*NPR1*	−0.494	0.001	−1.783	0	−0.389	0.001	−0.074	0.287	NONEXPRESSOR OF PR GENES1
At5g45110	*NPR3*	−1.024	0.009	−1.869	0.006	–	n/a	–	n/a	NPR1-LIKE PROTEIN3
At4g19660	*NPR4*	–	n/a	−1.435	0.006	–	n/a	–	n/a	NPR1-LIKE PROTEIN4
At4g16890	*SNC1*	–	n/a	−2.361	0	–	n/a	–	n/a	SUPPRESSOR OF NPR1-1, CONSTITUTIVE 1
At1g02450	*NIMIN1*	–	n/a	−3.318	0.017	–	n/a	1.142	0.002	NIM-INTERACTING1
At3g25882	*NIMIN2*	–	n/a	−2.493	0.034	−1.099	0.001	–	n/a	NIM-INTERACTING2
At1g74710	*ICS1*	–	n/a	−4.154	0.001	–	n/a	–	n/a	ISOCHORISMATE SYNTHASE1
At4g39030	*EDS5*	–	n/a	−3.815	0.003	–	n/a	–	n/a	ENHANCED DISEASE SUSCEPTIBILITY5
At5g13320	*PBS3*	–	n/a	−3.979	0.008	–	n/a	–	n/a	AVRPPHB SUSCEPTIBLE3
At3g48090	*EDS1*	–	n/a	−2.208	0.007	–	n/a	–	n/a	ENHANCED DISEASE SUSCEPTIBILITY1
At3g52430	*PAD4*	–	n/a	−3.458	0.003	–	n/a	1.257	0.002	PHYTOALEXIN DEFICIENT4
At5g14930	*SAG101*	–	n/a	−1.055	0.013	–	n/a	–	n/a	SENESCENCE-ASSOCIATED GENE101
At4g23570	*SGT1A*	–	n/a	−3.091	0	–	n/a	1.001	0.003	Suppressor of G2 (Two) 1A
At4g14400	*ACD6*	−2.818	0.023	−3.125	0.011	−1.368	0	–	n/a	ACCELERATED CELL DEATH6
At2g13810	*ALD1*	–	n/a	−4.106	0.002	−3.129	0.002	−2.105	0	AGD2-LIKE DEFENSE RESPONSE PROTEIN1
At1g19250	*FMO1*	–	n/a	−4.486	0.004	−2.561	0.005	−1.447	0.001	FLAVIN_DEPENDENT MOMOOXYGENASE1
NPR1 target genes										
At2g14610	*PR1*	−1.024	0.174	2.325	0.151	−6.469	0	−3.246	0.001	PATHOGENESIS-RELATED GENE1
At3g57260	*PR2*	−2.147	0.18	–	n/a	−1.93	0	−2.347	0.008	PATHOGENESIS-RELATED GENE2
At1g75040	*PR5*	−1.37	0	−1.334	0.23	−1.924	0	–	n/a	PATHOGENESIS-RELATED GENE5
At2g43570	n.a.	−2.185	0.131	–	n/a	−1.882	0.002	–	n/a	Chitinase, putative
At4g12010	n.a.	–	n/a	−1.31	0.006	–	n/a	–	n/a	Disease resistance protein, putative
At4g34480	n.a.	–	n/a	–	n/a	−1.01	0.003	–	n/a	Glycosyl hydrolase family 17 protein
At5g43470	*RPP8*	–	n/a	−1.14	0.003	–	n/a	–	n/a	RECOGNITION OF PERONOSPORA PARASITICA8
At5g57550	*XTR3*	−1.77	0.001	1.332	0.018	1.362	0	1.256	0.015	XYLOGLUCAN ENDOTRANSGLYCOSYLASE3
At1g08450	*CRT3*	–	n/a	−1.653	0.003	−1.293	0	–	n/a	CALRETICULIN 3; calcium ion binding
At1g09210	*CRT2*	–	n/a	–	n/a	−1.755	0	–	n/a	Calreticulin2
At1g30900	*VSR6*	–	n/a	−2.128	0.023	−1.8	0	–	n/a	Vacuolar sorting receptor6
At2g34250	*Sec61*α	–	n/a	–	n/a	−1.161	0.106	–	n/a	Protein transport protein, putative
At2g47470	*PDIL2-1*	–	n/a	–	n/a	−1.235	0	–	n/a	PDI-LIKE2-1; thiol-disulfide exchange intermediate
At4g22670	*HIP1*	–	n/a	–	n/a	−1.084	0.029	–	n/a	HSP70-INTERACTING PROTEIN1; binding
At4g24190	*SHD*	–	n/a	–	n/a	−1.801	0	–	n/a	SHEPHERD; ATP binding
At5g07340	n.a.	–	n/a	–	n/a	−1.548	0.007	–	n/a	Calnexin, putative
At5g42020	*BIP*	–	n/a	–	n/a	−1.978	0.001	–	n/a	LUMINAL BINDING PROTEIN; ATP binding
At5g61790	*CNX1*	–	n/a	–	n/a	−1.878	0	–	n/a	Calnexin 1
At4g31800	*WRKY18*	−1.377	0.012	–	n/a	–	n/a	–	n/a	WRKY DNA binding protein 18
At5g22570	*WRKY38*	−1.34	0.088	–	n/a	−1.301	0.001	–	n/a	WRKY DNA binding protein 38
At4g23810	*WRKY53*	−1.144	0.006	−1.777	0.004	–	n/a	–	n/a	WRKY DNA binding protein 53
At2g40750	*WRKY54*	−1.781	0.022	−3.326	0.002	–	n/a	–	n/a	WRKY DNA binding protein 54
At3g01080	*WRKY58*	–	n/a	–	n/a	−1.374	0	–	n/a	WRKY DNA binding protein 58
At2g21900	*WRKY59*	–	n/a	−1.926	0	−1.714	0	1.335	0.004	WRKY DNA binding protein 59
At1g80590	*WRKY66*	–	n/a	–	n/a	−1.365	0.005	–	n/a	WRKY DNA binding protein 66
At3g56400	*WRKY70*	−1.666	0.021	−2.197	0.024	–	n/a	–	n/a	WRKY DNA binding protein 70

AGI, Arabidopsis Genome Initiative; FC, fold change; n.a., not available; n/a, not applicable; –, less than twofold.

Although some methylcytosines were identified in only one genotype, the majority (72.8%) of the methylcytosines in all sequence contexts (CG, CHG, and CHH) were identified in both *elp2* and the wild type (see Supplemental Figure 4 online). The average methylation levels of methylcytosines in the CG, CHG, and CHH contexts in *elp2* were 5.94, 1.27, and 2.34% lower than those in the wild type, respectively (Figure 5A). In all sequence contexts, significantly more methylcytosines in *elp2* displayed a low percentage (<10%) of methylation than in the wild type (Figures 5B to 5D). However, although the distribution

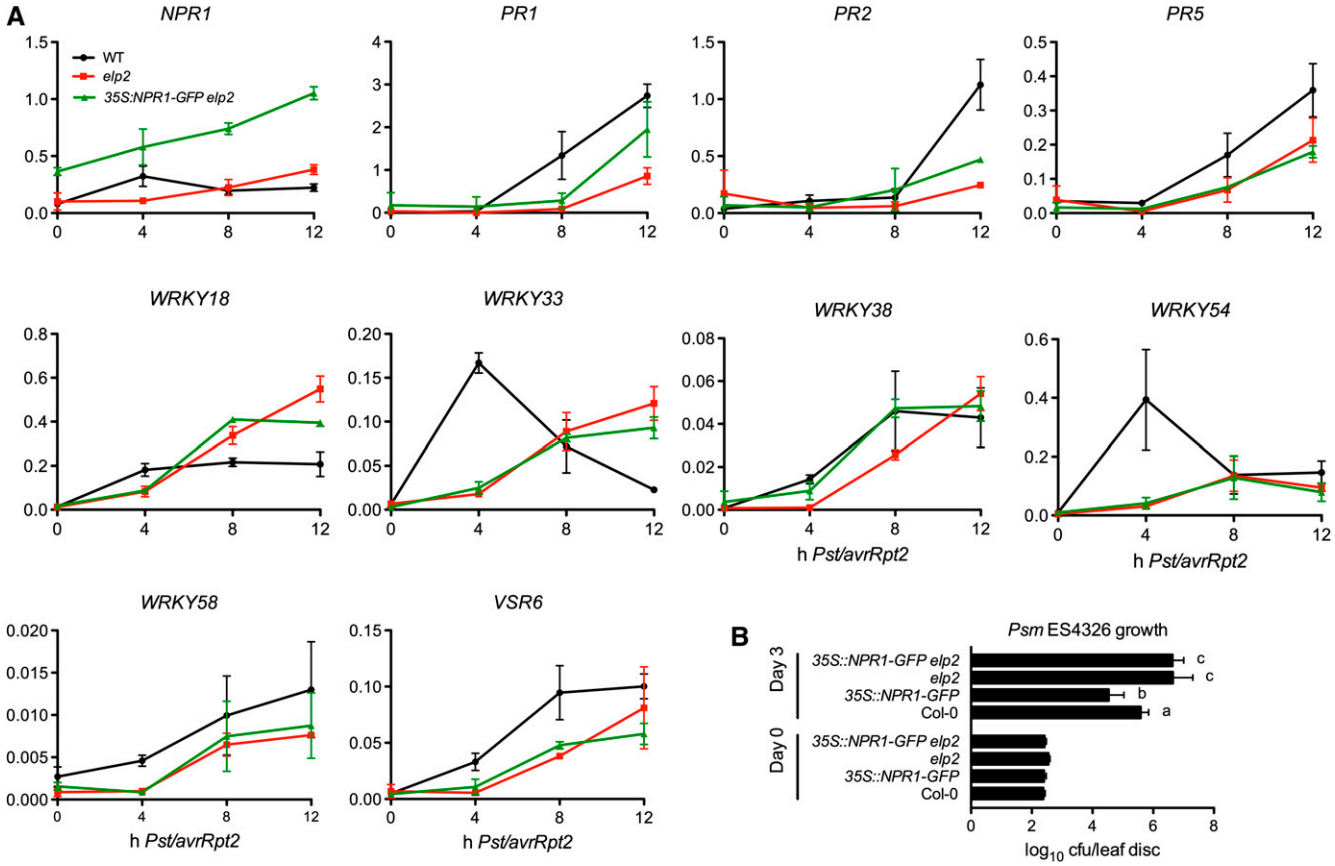

Figure 2. Epistasis between *elp2* and the *35:NPR1-GFP* Transgene

(A) Expression of *NPR1* and nine NPR1 target genes in *Pst* DC3000/*avrRpt2*-infected wild-type (WT), *elp2*, and *35S:NPR1-GFP elp2* plants. The *y* axes indicate relative expression levels. Expression levels were monitored using qPCR and normalized against *UBQ5*. The *x* axes indicate hours after *Pst* DC3000/*avrRpt2* infection. Data represent the mean of three independent samples with SD.

(B) Growth of *Psm* ES4326 in wild-type, *elp2*, and *35S:NPR1-GFP elp2* plants. Data represent the mean of eight independent samples with SD. Different letters on the right of the bars indicate significant differences ($P < 0.05$, *t* test).

Experiments were repeated three times with similar results.

patterns of methylcytosine were similar in *elp2* and the wild type (see Supplemental Figure 5 online), more methylcytosines were identified in *elp2* than in the wild type (see Supplemental Figures 4 and 5 online). Methylcytosine differences between *elp2* and the wild type were evident in all sequence contexts with more prominent differences being identified in the CHG and CHH contexts (see Supplemental Figure 5 online). The hypermethylated regions in *elp2* were evenly distributed along the chromosomes except for the centromeric regions (see Supplemental Figure 5 online). We scanned the methylcytosines on chromosome 1 and identified several regions where DNA methylation levels in *elp2* and the wild type differed significantly (Figures 5E and 5F). In each of these regions, the patterns of DNA methylation in all sequence contexts varied dramatically between *elp2* and the wild type (Figures 5G to 5L). We observed that the DNA methylation pattern of *PAD4* revealed by the genome-wide BS-Seq was similar to that detected by traditional bisulfite sequencing (Figure 4D; see Supplemental Figure 6 online), which validated the BS-Seq method employed in this study. Taken together, our results showed that the *elp2* mutation increased the total number of methylcytosines, decreased average methylation levels of methylcytosines, and modulated (either increased or decreased) methylation levels of specific cytosines, suggesting that ELP2 is an epigenetic regulator modulating both DNA demethylation and methylation.

ELP2 Is Required for Pathogen-Induced Dynamic DNA Methylation Changes in *NPR1* and *PAD4*

Pathogen infection has been shown to cause DNA hypomethylation in *Arabidopsis* (Pavet et al., 2006; Agorio and Vera, 2007; Dowen et al., 2012). Since ELP2 modulates basal DNA methylation levels, we asked whether ELP2 is involved in pathogen-induced DNA methylation changes. To address this question, we infected *elp2* and wild-type leaves with *Pst* DC3000/*avrRpt2* and analyzed DNA methylation in *NPR1* and *PAD4* at 0, 4, 8, 16, and 24 hpi. Surprisingly, during the first 24 h after *Pst* DC3000/*avrRpt2* infection, DNA methylation levels

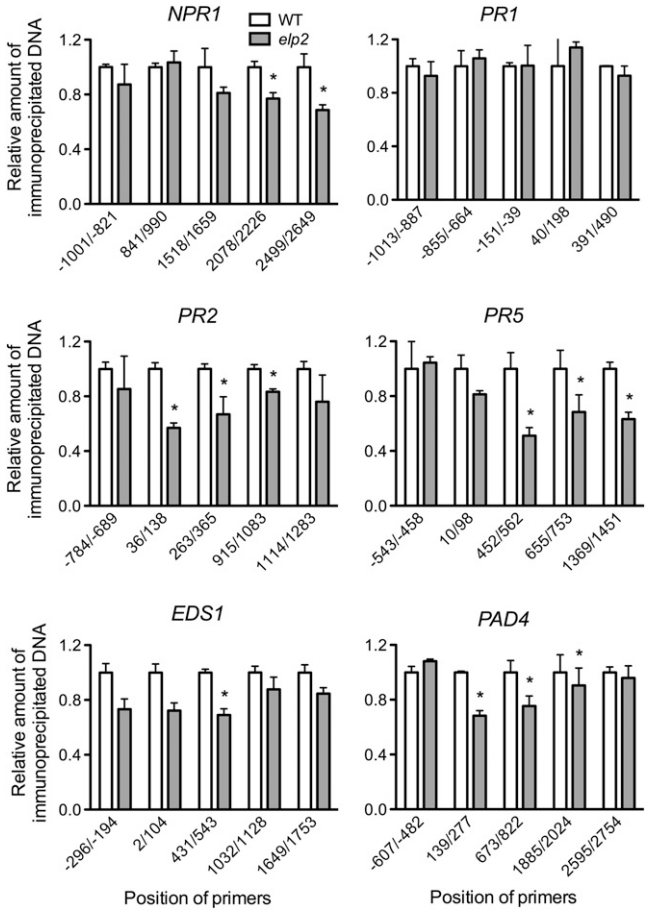

Figure 3. Histone H3 Acetylation Levels in Several Defense Genes.

The position of the primers is relative to the initiation ATG codon. The relative amount of immunoprecipitated chromatin fragments (as determined by real-time qPCR) from *elp2* was compared with that from the wild type (WT; arbitrarily set to 1). Data represent the mean of three independent samples with SD. An asterisk indicates a significant difference between *elp2* and the wild type ($P < 0.05$, *t* test). The experiment was repeated four times with similar results.

changed dramatically in the wild type but remained relatively high and stable in *elp2* (Figure 6; see Supplemental Figure 7 online). The most dramatic changes in DNA methylation levels occurred at the CG sites in the *PAD4* coding region (Figure 6D; see Supplemental Figures 7J to 7L online). The overall average methylation level of the eleven CG sites in the sequenced *PAD4* coding region increased from ~56.7% at 0 hpi to ~69.2% at 4 hpi, then dropped to ~60.1, ~48.9, and ~47.7% at 8, 16, and 24 hpi, respectively (Figure 6D). At the *PAD4* C2612G site, the methylation level increased from ~50.2% at 0 hpi to ~75.9% at 4 hpi, then dropped to ~64.7, ~24.6, and ~14.4% at 8, 16, and 24 hpi, respectively (see Supplemental Figure 7K online). In the *NPR1* promoter region, methylation levels at CG and CHG sites increased and reached the highest levels at 16 hpi, then decreased slightly at 24 hpi (Figures 6A and 6B; see Supplemental Figures 7A to 7F online), whereas methylation levels at CHH sites were low and did not display any reproducible dynamic patterns (Figure 6C; see Supplemental Figures 7G to 7I online). Taken together, these results indicate that ELP2 contributes to pathogen-induced dynamic changes in DNA methylation levels of two major defense genes.

DISCUSSION

Elongator has been implicated in diverse biological processes, including exocytosis, embryogenesis, cell migration, cell proliferation, and responses to abiotic stresses (Nelissen et al., 2005; Rahl et al., 2005; Chen et al., 2006; Close et al., 2006; Creppe et al., 2009; Okada et al., 2010; Bauer et al., 2012). Our previous characterization of the *Arabidopsis elp2* mutant uncovered a role for Elongator in plant immune responses (DeFraia et al., 2010). We showed that *elp2* mutations delay or/and decrease the induction of several defense genes, but the underlying mechanism remains unclear. Here, we provide evidence that ELP2 functions in DNA demethylation/methylation and histone acetylation and is involved in plant immunity by directly or indirectly affecting the kinetics of pathogen-induced transcriptome reprogramming.

Induction of many defense genes is delayed in the *elp2* mutant (Figure 1E). Similar expression patterns were observed for several stress-inducible genes in yeast *elp*Δ cells (Otero et al., 1999). Expression of *GAL1-10*, *PHO5*, and *ENA1* is delayed in *elp*Δ cells following transfer to media containing Gal, low phosphate, and high salt, respectively. Although these results clearly showed that Elongator is involved in regulating the expression kinetics of individual stress-inducible genes, whether Elongator governs the kinetics of stress-induced transcriptome changes is not yet known. Our results suggest that Elongator plays a critical role in shaping the kinetics of pathogen-induced transcriptome changes. Compared with the *npr1* mutation, *elp2* has a much stronger impact on the kinetics of pathogen-induced transcriptional reprogramming (Figure 1C). The *npr1* mutation does not dramatically change the numbers of genes that are up- or downregulated after *Pst* DC3000/*avrRpt2* infection, whereas *elp2* significantly reduces the gene numbers at early time points. The numbers of genes that are up- or downregulated in *elp2* reach higher levels at a later time point compared with the wild type and *npr1*, suggesting that *elp2* delays genome-wide transcriptional responses to pathogen infection. These results, together with the pathogen susceptibility phenotype of *elp2*, indicate that ELP2 is required for the *Arabidopsis* genome to rapidly and efficiently reprogram its transcriptome to fend off pathogen attack.

ELP2 regulates the expression of a group of major defense genes, including *NPR1*, *EDS1*, *PAD4*, *EDS5*, *ICS1*, *NDR1*, *ALD1*, and *FMO1* (Table 1, Figure 1E) (Cao et al., 1997; Century et al., 1997; Falk et al., 1999; Jirage et al., 1999; Wildermuth et al., 2001; Nawrath et al., 2002; Song et al., 2004; Mishina and Zeier, 2006), which suggests that ELP2 may regulate plant immune responses through these major defense genes. ELP2 may also function independently of these genes, as seen for *NPR1*. In the NPR1 transcriptional cascade, ELP2 not only regulates *NPR1* itself, but also regulates almost all of the NPR1 target genes

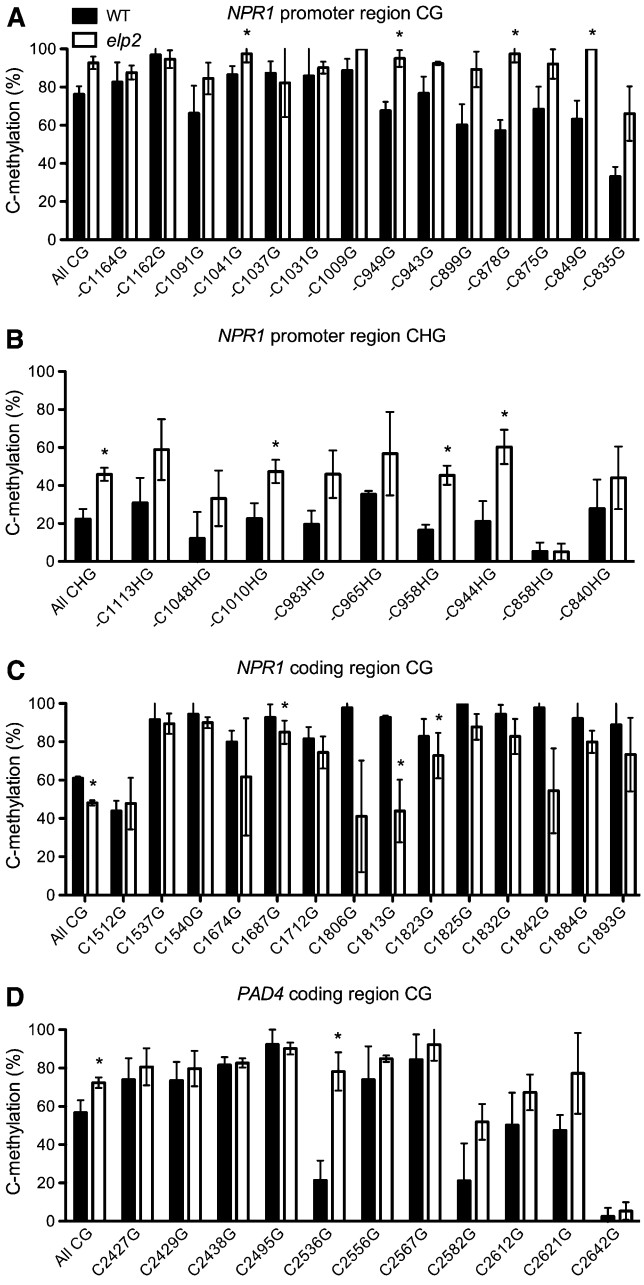

Figure 4. DNA Methylation Levels in Several Defense Genes.

(A) and **(B)** DNA methylation levels at CG sites **(A)** and CHG sites **(B)** of the *NPR1* promoter region in *elp2* and the wild type (WT).

(C) and **(D)** DNA methylation levels at CG sites in the coding region of *NPR1* **(C)** and *PAD4* **(D)** in *elp2* and the wild type.

DNA samples were extracted from three biological replicates of each genotype. After bisulfite conversion and PCR amplification, the PCR products were cloned into pGEM-T easy vector. A total of 45 independent clones were sequenced for each genotype (15 for each DNA sample). The 15 clones from the same DNA sample were used to calculate methylation levels, which were then used for statistical analysis. Data represent the mean of three independent samples with SD. An asterisk indicates a significant difference between *elp2* and the wild type ($P < 0.05$, *t* test).

(Table 1) (Wang et al., 2005). Overexpression of the previously characterized transgene *NPR1-GFP* in *elp2* does not restore the induction pattern of most of the NPR1 target genes tested in our experiment (Figure 2A) (Kinkema et al., 2000), indicating that ELP2 also functions independently of NPR1 and is involved in the transcription activation of NPR1 target genes. Consistently, increasing basal immunity by overexpression of *NPR1-GFP* requires ELP2 (Figure 2B) (Cao et al., 1998). Thus, in NPR1-mediated signal transduction, ELP2 functions in a transcriptional feed-forward loop, in which it regulates both *NPR1* and its target genes.

Although ELP2 regulates the NPR1 transcriptional cascade, ELP2 and NPR1 appear to function largely independently of each other in effector-triggered immunity (ETI) (DeFraia et al., 2010). This paradox can be reconciled by the fact that other ELP2-regulated major defense genes, such as *PAD4*, *EDS1*, and *NDR1*, influence subsets of NPR1-independent genes (Wang et al., 2008). Mutations in *ELP2* delay the induction of both NPR1-dependent and -independent defense genes, whereas mutations in *NPR1* block the transcription of only NPR1-dependent defense genes. Our previous work has shown that the *elp2* and *npr1* single mutants are moderately susceptible to *Pst* DC3000/*avrRpt2*, whereas the *elp2 npr1* double mutant is significantly (>130-fold) more susceptible than either *elp2* or *npr1* (DeFraia et al., 2010). Therefore, both ELP2-regulated kinetics and the NPR1-dependent magnitude of defense gene induction are crucial for ETI. Intriguingly, although ELP2 regulates the induction kinetics of a group of major defense genes that encode important regulators of systemic acquired resistance (SAR) (Table 1), ELP2 itself does not play a significant role in SAR (DeFraia et al., 2010). It is possible that the basal expression levels of the major defense genes, which are not affected by the *elp2* mutation (see Supplemental Figure 2 online), are sufficient for the establishment of SAR, as shown for the *NPR1* gene (van Wees et al., 2000). It is also possible that establishment of SAR does not depend on the kinetics of defense gene induction, but rather on the magnitude of the induction. In any case, *elp2*, as a unique mutant in which both basal immunity and ETI are compromised but SAR is not, is invaluable for dissecting the mechanistic differences between basal immunity or ETI and SAR (DeFraia et al., 2010).

It has been well documented that Elongator possesses HAT activity and is required for maintaining normal histone acetylation levels (Winkler et al., 2002; Close et al., 2006; Nelissen et al., 2010). Consistent with this, loss of ELP2 reduces basal histone acetylation levels in the coding regions of several defense genes (Figure 3). Elongator might also bear DNA demethylase activity, affecting paternal genome demethylation in mouse zygotes (Okada et al., 2010). However, it is unknown whether Elongator influences DNA demethylation in somatic cells and whether this function is conserved in other organisms. In this study, we found that *elp2* causes dramatic genome-wide DNA methylation changes, including increased total number of methylcytosines (Figure 5; see Supplemental Figures 4 and 5 online). These changes appear to be more profound than those observed in the DNA demethylase triple mutant *rdd*, in which the total number of methylcytosines identified is similar to the wild type (Lister et al., 2008). Many regions in *elp2* exhibit increased DNA methylation

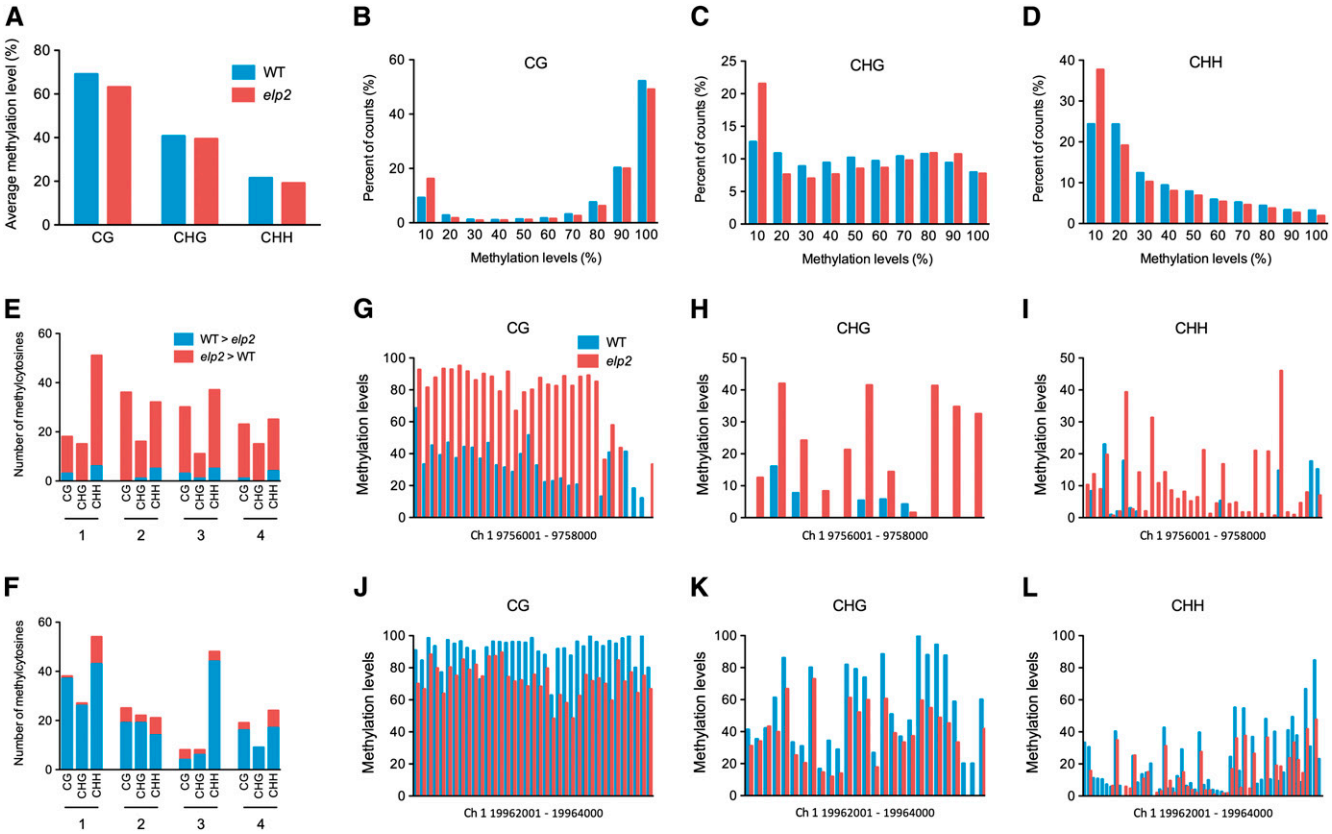

Figure 5. Genomic DNA Methylation Profiles of *elp2*.

(A) Average genome-wide DNA methylation levels of *elp2* and the wild type (WT).
(B) to **(D)** Distribution of methylation percentage in the sequence context of CG **(B)**, CHG **(C)**, and CHH **(D)** in *elp2* and the wild type The *x* axes are divided into 10 individual bins that correspond to methylation levels. The *y* axes are the percentage of total counts for each respective bin.
(E) and **(F)** Regions on chromosome 1 where more methylcytosines are hypermethylated in either *elp2* **(E)** or the wild type **(F)**. Regions 1 to 4 correspond to nucleotides 8,390,001 to 8,392,000, 568,001 to 570,000, 9,756,001 to 9,758,000, and 3,876,001 to 3,878,000, respectively **(E)**, or nucleotides 19,962,001 to 1,996,400, 11,318,001 to 11,320,000, 16,434,001 to 16,436,000, and 27,932,001 to 27,934,000, respectively **(F)**.
(G) to **(L)** Methylation levels of the methylcytosines in all sequence contexts in two regions on chromosome 1.

levels (Figures 5E and 5G to 5I), but some regions are hypomethylated (Figures 5F and 5J to 5L). This result suggests that, similarly to the human DNA methyltransferases Dnmt3a and 3b, Elongator may act in both DNA demethylation and methylation (Métivier et al., 2008). However, presently, no evidence is available indicating that Elongator acts upon DNA as a DNA demethylase or a DNA methyltransferase (Okada et al., 2010). This aspect of Elongator requires further investigation.

Methylation of genomic DNA in *Arabidopsis* is thought to be dynamically regulated by both active DNA demethylation and DNA methylation mechanisms (He et al., 2011). Consistent with this idea, we found that *Pst* DC3000/*avrRpt2* infection induces biphasic changes in DNA methylation levels in the *PAD4* coding region and, to a lesser extent, the *NPR1* promoter region in mature mesophyll cells in the wild type (Figure 6; see Supplemental Figure 7 online). However, DNA methylation levels of these regions in *elp2* are high (higher than the highest levels reached in the wild type) and do not change upon *Pst* DC3000/*avrRpt2* infection. Since mature mesophyll (nondividing somatic) cells cannot lose methylation through the loss of maintenance, this result indicates that the *elp2* mutation blocks pathogen infection-induced active DNA demethylation. Therefore, Elongator regulates genomic DNA methylation landscape likely through its DNA demethylation function in *Arabidopsis*.

Consistent with the notion that acetylation of histones H3 is generally associated with active transcription (Li et al., 2007), reduced histone H3 acetylation levels in the coding regions of several defense genes, including *NPR1* and *PAD4*, are correlated with delayed or/and decreased induction in *elp2* (Figures 1E and 3). Although basal expression levels of these defense genes are not significantly changed in the *elp2* mutant (see Supplemental Figure 2 online), a correlation between reduced histone H3 acetylation and decreased basal expression of several auxin-related genes has been seen in the *Arabidopsis* Elongator mutant *elo3-6* (Nelissen et al., 2010). Therefore, Elongator may help establish a transcriptionally active chromatin state at specific defense loci. A role for histone modification in establishment of active chromatin structures at plant defense

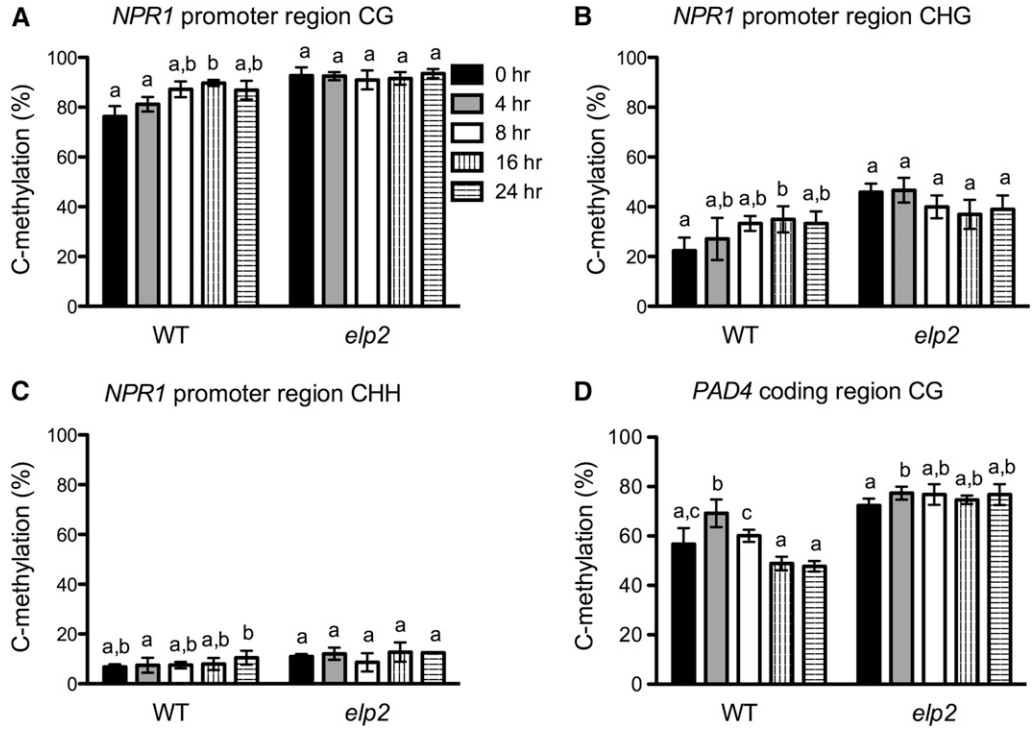

Figure 6. Pathogen-Induced Dynamic DNA Methylation Changes in *NPR1* and *PAD4*.

(A) to **(C)** Average methylation levels of methylcytosines at CG sites **(A)**, CHG sites **(B)**, and CHH sites **(C)** of the *NPR1* promoter region in *elp2* and the wild type (WT).

(D) Average methylation levels of methylcytosines at CG sites of the *PAD4* coding region in *elp2* and the wild type.

DNA samples were extracted from three biological replicates of each genotype/time point. After bisulfite conversion and PCR amplification, the PCR products were cloned into pGEM-T easy vector. A total of 45 independent clones were sequenced for each genotype/time point (15 for each DNA sample). The 15 clones from the same DNA sample were used to calculate methylation levels, which were then used for statistical analysis. Data represent the mean of three independent samples with SD. Different letters above the bars indicate significant differences ($P < 0.05$, *t* test). Note that the comparison was made separately among time points for each genotype.

loci is not without precedent. The *Arabidopsis* histone methyltransferase SET DOMAIN GROUP8 maintains H3K36me3 levels and regulates both basal and induced expression of particular *R* genes (Palma et al., 2010). *ARABIDOPSIS* HOMOLOG OF TRITHORAX1 establishes H3K4me3 patterns and regulates both basal and induced expression of *WRK70*, which encodes a key transcription factor of plant immunity (Li et al., 2006; Alvarez-Venegas et al., 2007). Histone modification may even be a molecular basis for defense priming, a phenomenon resulting in enhanced defense gene transcription upon a subsequent stress (Conrath, 2011; Berr et al., 2012). Indeed, priming of *WRKY6*, *WRKY29*, and *WRKY53* is associated with an increase in histone H3 acetylation and H3K4me3 at their promoters (Jaskiewicz et al., 2011). Although ELP2 does not contribute significantly to the establishment of SAR (DeFraia et al., 2010), whether Elongator is involved in priming-mediated histone acetylation deserves further investigation.

Interestingly, besides histone acetylation, DNA methylation levels are elevated in the *NPR1* promoter region and the *PAD4* coding region in *elp2* plants (Figure 4), which may also contribute to the delayed or/and decreased induction. Furthermore, we found that pathogen-induced dynamic changes in DNA methylation levels in the *PAD4* coding region and, to a lesser extent, the *NPR1* promoter region are correlated with the impulse response of the genes to pathogen infection (Figures 1E and 6; see Supplemental Figure 7 online). Dynamic DNA methylation changes have previously been implicated in regulation of gene transcription. During mouse muscle cell line differentiation, the dynamics of DNA demethylation in the 5′-flanking region and exon 1 of the *myogenin* gene is strongly correlated with its expression (Lucarelli et al., 2001). In human MDA-MB231 cells, transcriptional regulation of the human *pS2* gene involves cyclical variation in CG methylation of the *pS2* promoter (Métivier et al., 2008). The *elp2* mutation blocks pathogen-induced DNA methylation changes in *NPR1* and *PAD4* and delays the induction of the defense genes, suggesting that, in *Arabidopsis*, pathogen-induced Elongator-dependent dynamic DNA methylation changes may play a role in regulating defense gene transcription.

Compared with other epigenetic regulators, Elongator is unique in that it regulates both global histone acetylation levels and genome-wide DNA methylation profiles (Figure 5) (Winkler et al., 2002; Nugent et al., 2010; Xu et al., 2012). The delayed genome-wide transcriptional response of *elp2* to pathogen infection

likely results from altered genome chromatin structure caused by both reduced histone acetylation levels and altered DNA methylation profiles. Proteins regulating global histone acetylation or/and genome-wide DNA methylation have been implicated in plant innate immunity. For instance, the *Arabidopsis* HISTONE DEACETYLASE19 (HDA19) appears to be involved in basal defense against the bacterial pathogen *Pst* DC3000 but results from examining the effect of *hda19* mutations on disease resistance in several reports are contradictory (Tian et al., 2005; Kim et al., 2008; Choi et al., 2012). Knockout of *SIRTUIN2*, a homolog of yeast *Silent information regulator2*, which encodes an NAD^+-dependent HDA, enhances resistance to *Pst* DC3000 (Wang et al., 2010). Mutations in several components of the RNA-directed DNA methylation pathway have been shown to alter immune responses to *Pst* DC3000. While mutations in *AGRONAUTE4* (*AGO4*) compromise resistance to *Pst* DC3000 (Agorio and Vera, 2007), mutations in *NRPE1* and *NRPD2*, which encode the largest subunit of the RNAP V complex and second largest subunit of the RNAP IV and V complexes, respectively (Law and Jacobsen, 2010), enhance resistance to this pathogen (López et al., 2011). The DNA methylation mutants *met1-3* and *ddc* (*drm1-2 drm2-2 cmt3-11*), which are deficient in CG maintenance methylation and non-CG maintenance/de novo methylation, respectively (Saze et al., 2003; Chan et al., 2006; Penterman et al., 2007a), are highly resistant to *Pst* DC3000 (Dowen et al., 2012; Luna et al., 2012). As AGO4 might play some unknown functions independent of the RNA-directed DNA methylation pathway (López et al., 2011), it has been proposed that DNA methylation represses immune responses to *Pst* DC3000 in the absence of the pathogen (Dowen et al., 2012). However, we found that the DNA demethylase triple mutant *rdd* (*ros1-3 dml2-1 dml3-1*), which contains genome-wide DNA hypermethylation (Penterman et al., 2007b; Lister et al., 2008), also exhibits constitutively elevated resistance to bacterial pathogens (see Supplemental Figure 8 online). Therefore, changing global histone acetylation levels or/and genomic DNA methylation profiles exerts great influence on plant immune responses. Interestingly, although both *elp2* and *rdd* are DNA demethylation mutants, their defense phenotypes are opposite (see Supplemental Figure 8 online) (DeFraia et al., 2010). The enhanced disease susceptibility of *elp2* might be attributed to impaired histone acetylation. Although the intrinsic relationship between histone acetylation and DNA demethylation/methylation in *elp2* is unknown, it would be interesting to test whether histone acetylation is epistatic to DNA methylation in plant immune responses. Furthermore, recent studies have shown that HDA6 and MET1 interact directly and function together in locus-directed heterochromatin silencing (To et al., 2011; Liu et al., 2012). Whether Elongator counteracts HDA/DNA methyltransferase complexes in epigenetic regulation of plant immunity merits further investigation.

Elongator employs distinct molecular mechanisms to play diverse functions in different biological processes (Svejstrup, 2007; Versées et al., 2010). Our data revealed a new role for Elongator in regulating DNA demethylation/methylation in non-dividing somatic cells and demonstrated an important function for Elongator-mediated chromatin regulation in plant immune responses, though this function could be direct or indirect. We propose that Elongator plays a key role in genome-wide transcriptomic responses to diverse stresses, likely by regulating the histone acetylation and DNA methylation status of stress-responsive genes. The NPR1 transcriptional cascade exemplifies a signaling cascade where Elongator modulates the chromatin structure of both the key transcription regulator and its target genes, forming a transcriptional feed-forward loop and determining the kinetics of the transcription. Further investigation on the relationship between NPR1 and Elongator in regulating gene transcription during immune responses will shed light on the cooperative interaction between specific transcription regulators and chromatin structure.

METHODS

Plant Materials and Pathogen Infection

The wild type used was the *Arabidopsis thaliana* Columbia-0 (Col-0) ecotype, and the mutant alleles used were *npr1-3* (Glazebrook et al., 1996), *elp2-5* (DeFraia et al., 2010), *met1-3* (Saze et al., 2003), *drm1-2 drm2-2 cmt3-11* (Chan et al., 2006), and *ros1-3 dml2-1 dml3-1* (Penterman et al., 2007b). The *35S:NPR1-GFP* transgenic line has been described previously (Kinkema et al., 2000). Plant growth, pathogen infection, and determination of in planta pathogen growth were performed as previously described (Cao et al., 1997).

RNA Analysis

RNA extraction, reverse transcription, and real-time qPCR analysis were performed as described by DeFraia et al. (2010). The primers used for real-time qPCR in this study are shown in Supplemental Table 3 online.

Microarray Analysis

Four-week-old soil-grown plants were inoculated with the bacterial pathogen *Pst* DC3000/*avrRpt2*. Total RNA samples extracted from the inoculated leaves were subjected to microarray analysis. Briefly, RNA concentration was determined on a NanoDrop Spectrophotometer (Thermofisher Scientific), and sample quality was assessed using the 2100 Bioanalyzer (Agilent Technologies). cDNA was synthesized from 200 ng of total RNA and used as a template for in vitro transcription in the presence of T7 RNA polymerase and cyanine-labeled CTPs using the Quick Amp Labeling kit (Agilent Technologies) according the manufacturer's protocol. The amplified, labeled complementary RNA was purified using the RNeasy mini kit (Qiagen). For each array, 1650 ng of Cy 3–labeled complementary RNA was fragmented and hybridized with rotation at 65°C for 17 h. Samples were hybridized to *Arabidopsis* 4 × 44k arrays (Agilent Technologies). The arrays were washed according to the manufacturer's protocol and then scanned on a G2505B scanner (Agilent Technologies). Data were extracted using Feature Extraction 10.1.1.1 software (Agilent Technologies).

Data (individual signal intensity values) obtained from the microarray probes were background corrected using a *normexp+offset* method, in which a small positive offset ($k = 50$) was added to move the corrected intensities away from zero (Ritchie et al., 2007). The resulting data were log transformed (using 2 as the base) and normalized between individual samples by scaling the individual log-transformed signal intensities so that all data sets had comparable lower quartile, median, and upper quartile values (Smyth, 2005). After normalization, the Student's *t* test was performed considering a probe-by-probe comparison between different genotypes at the same time point using the wild type (Col-0) as the reference sample and between different time points of the same genotype

using the 0-h sample as the reference. In each comparison, a P value and fold change were computed for each gene locus. The gene expression fold changes were computed based on the normalized log-transformed signal intensity data. The comparison results were further explored to obtain numbers of overlapped genes between/among different comparisons.

Chromatin Immunoprecipitation

Chromatin immunoprecipitation was performed as described by Saleh et al. (2008). Briefly, ~3 g of 4-week-old soil-grown plants were submerged in 50 mL of cross-linking buffer (10 mM Tris-HCl, pH 8, 0.4 M Suc, 1 mM PMSF, 1 mM EDTA, and 1% formaldehyde) and vacuum infiltrated three times for 3 to 4 min each at room temperature. The cross-linking reaction was stopped by adding 2.5 mL of 2 M Gly to a final concentration of 100 mM and vacuum infiltration for 5 min. Plant tissues were washed three times with cold sterile deionized water. After removing water, plants tissues were submerged in liquid nitrogen, ground to a fine powder, and resuspended in 20 to 25 mL cold nuclei isolation buffer (15 mM PIPES, pH 6.8, 0.25 M Suc, 5 mM $MgCl_2$, 60 mM KCl, 15 mM NaCl, 1 mM $CaCl_2$, 0.9% Triton X-100, 20 mM sodium butyrate, 1 mM PMSF, 2 μg/mL pepstatin A, and 2 μg/mL aprotinin). After brief vortex and incubation, the homogenized slurry was filtered through one layer of Miracloth. After centrifugation at 3220*g* for 20 min, the pellet (nuclei) was resuspended in 1.5 mL of cold nuclei lysis buffer (50 mM HEPES, pH 7.5, 150 mM NaCl, 1 mM EDTA, 0.1% SDS, 0.1% sodium deoxycholate, 1% Triton X-100, 20 mM sodium butyrate, 1 μg/mL pepstatin A, and 1 μg/mL aprotinin). DNA was sheared into ~500-bp (200 to 1000 bp) fragments by 6 to 10 min of 3-s pause sonication at 40 to 43% amplitude using a TekMar TM-100 sonic disruptor (TekMar). After centrifugation at 13,800*g* for 10 min, the supernatant (200 μL) was diluted fivefold with nuclei lysis buffer and precleared by adding 50 μL salmon sperm DNA/protein A agarose beads. After removing the agarose beads, 5 μL of Ac-Histone H3 (Lys-9/14) antibody (sc-8655-R; Santa Cruz Biotechnology) was added and the mixture was incubated at 4°C for 5 h to overnight with gentle rotation, and then 60 to 75 μL salmon sperm DNA/protein A agarose beads was added and the incubation was continued for 2 to 3 h. After centrifugation at 3800*g* for 2 min, the agarose beads were sequentially washed with low salt wash buffer (20 mM Tris-HCl, pH 8, 150 mM NaCl, 0.2% SDS, 0.5% Triton X-100, and 2 mM EDTA), high salt wash buffer (20 mM Tris-HCl, pH 8, 500 mM NaCl, 0.2% SDS, 0.5% Triton X-100, and 2 mM EDTA), LiCl wash buffer (10 mM Tris-HCl, pH 8, 0.25 M LiCl, 1% sodium deoxycholate, 1% Nonidet P-40, and 1 mM EDTA), and TE buffer (twice; 1 mM EDTA and 10 mM Tris-HCl, pH 8). The immunocomplexes were eluted with freshly prepared elution buffer (0.1 M $NaHCO_3$ and 0.5% SDS) and incubation at 65°C for 15 min with gentle rotation. Twenty microliters of 5 M NaCl was added to 500 μL of the immunocomplex solution and the mixture was incubated at 65°C for 4 h to overnight to reverse cross-linking. Then, 20 μL of 1 M Tris-HCl, pH 6.5, 10 μL of 0.5 M EDTA, and 2 μL proteinase K (10 mg/mL) was added, and the mixture was incubated at 45°C for 1.5 h to digest the proteins. Immunoprecipitated DNA was purified using a mixture of phenol:chloroform:isoamyl alcohol (25:24:1), and the resulting DNA was used for real-time qPCR with the primers in Supplemental Table 4 online. The amount of precipitated DNA corresponding to a specific gene region was determined by real-time qPCR and normalized to both input DNA and a constitutively expressed gene (*ACTIN2/7*) as described (Mosher et al., 2006). The resulting values were used as measures for the levels of histone H3K9/14ac in specific gene regions.

Bisulfite Sequencing

For locus-specific DNA methylation analysis, strand-specific and bisulfite-specific primers (see Supplemental Table 1 online) were used to amplify the target regions from bisulfite-converted genomic DNA. The PCR products were cloned into pGEM-T easy vector (Promega). Individual clones were sequenced, and the sequence data were analyzed using the Web-based tool Kismeth (http://katahdin.mssm.edu/kismeth) (Gruntman et al., 2008). Genome-wide bisulfite sequencing and data analysis were performed as described by Lister et al. (2008). Briefly, genomic DNA was extracted from ~1 g of fresh rosette leaves of 4-week-old soil-grown plants using a hexadecyltrimethylammonium bromide (CTAB) DNA extraction protocol (Aldrich and Cullis, 1993). Approximately 2 μg of high molecular weight genomic DNA was dissolved in 125 μL TE (10 mM Tris-HCl, pH 8.0, and 0.5 mM EDTA) and transferred to 6 × 16-mm glass microtubes with AFA fiber and snap-caps (Covaris). DNA samples were sheared into fragments with an average size of 300 bp in a Covaris S2 ultrasonic disruptor following the manufacturer's recommended settings. AMPure magnetic beads (Beckman Coulter) with a bead-to-sample ratio of 73:100 were used to clean up the samples prior to sequencing library construction. Sequencing libraries were made using the TruSeq DNA Sample Preparation kits (Illumina) following the manufacturer's protocol with a few modifications. Briefly, DNA fragments were end-repaired, adenylated, adaptor-ligated, and size-selected (250 to 500 bp) in a 2% agarose gel. The gel was stained with Invitrogen SYBR safe (Life Technologies) and viewed on a blue light transilluminator (Life Technologies) in order to avoid UV damage. Libraries were quantitated in a Qubit fluorometer (Life Technologies). The final yield was ~160 ng (in 25 μL Tris-HCl, pH 8.0), which was subjected to sodium bisulfite treatment using the EpiTect Bisulfite kit (Qiagen) following the manufacturer's instructions. The resulting library was amplified using uracil-insensitive PfuTurbo Cx Hotstart DNA polymerase (Agilent Technologies) under the following conditions: denaturation at 98°C for 30 s, 18 cycles (98°C for 15 s, 60°C for 30 s, and 72°C for 1 min), and final extension at 72°C for 5 min. The PCR amplification products were then cleaned twice using AMPure magnetic beads with a bead-to-sample ratio of 85:100, and the resulting DNA was quantitated by the Qubit fluorometer and qPCR with the Kapa SYBR Fast qPCR reagents (Kapa Biosystems) on an ABI7900HT real-time PCR system (Life Technologies). The average insert size of the libraries was ~360 bp. Libraries were then diluted to 9 pM for cluster generation on the cBOT (Illumina), and a 101 cycle multiplex single-end sequencing run for pooled barcoded libraries and a 2 × 101 cycle multiplex pair-end sequencing run for each library was performed on an Illumina Genetic Analyzer IIx (running SCS2.9) using an eight-lane flow cell.

The cleanup module of the Paracel Transcript Assembler version 3.0.0 was applied for raw reads cleanup. Consecutive ambiguous characters (Ns) were removed from both ends of a read, and all reads were checked and masked for adaptors. Low-quality sequences were trimmed from ends of individual reads, and reads with length shorter than 40 nucleotides were excluded from further analysis (see Supplemental Table 5 online). Reads were aligned against in silico bisulfite converted sense and antisense references of the *Arabidopsis* Col-0 genome and the nonconverted normal reference using the Novoalign software (Novocraft Technologies, V2.07.15b). A read was considered to be "mapped" to the sense reference if the number of mismatches with the antisense reference is at least twice that with the sense reference and vice versa. Mapped reads were filtered out as follows: reads either with three consecutive cytosines in CHH context (possible nonconversion in bisulfite conversion) or with mismatches more than 10% of the total nucleotides were removed (Bormann Chung et al., 2010; Otto et al., 2012); clonal reads potentially produced during PCR amplification from the same template molecule (based on a common start position) were removed. The uniquely mapped nonclonal reads were used for methylcytosine identification. A binomial probability distribution was used to calculate the minimum sequence depth at a cytosine position at which a methylcytosine could be called while maintaining a false positive rate below 5%. The false methylcytosine discovery rate was estimated by the sum of the rates of nonconversion

and thymidine to cytosine sequencing errors at cytosine positions in the chloroplast reference genome.

Statistical Methods

Except those used in microarray analysis, all statistical analyses were performed with the data analysis tools (*t* test: two samples assuming unequal variances) in Microsoft Excel of Microsoft Office 2004 for Macintosh.

Accession Numbers

Sequence data from this article can be found in the Arabidopsis Genome Initiative or GenBank/EMBL databases under the following accession numbers: ELP2 (At1g49540), NPR1 (At1g64280), EDS1 (At3g48090), PAD4 (At3g52430), EDS5 (At4g39030), ICS1 (At1g74710), NDR1 (At3g20600), FMO1 (At1g19250), ALD1 (At2g13810), PR1 (At2g14610), PR2 (At3g57260), PR5 (At1g75040), WRKY18 (At4g31800), WRKY33 (At2g38470), WRKY38 (At5g22570), WRKY54 (At2g40750), WRKY58 (At3g01080), and VSR6 (At1g30900); NCBI Gene Expression Omnibus Series number GSE38986 (microarray data); and NCBI Short Read Archive accession number SRA055073 (BS-Seq data).

Supplemental Data

The following materials are available in the online version of this article.

Supplemental Figure 1. *Pst* DC3000/*avrRpt2*-Induced Transcriptome Changes in *elp2*.

Supplemental Figure 2. Basal Expression Levels of Several Defense Genes in *elp2* and the Wild Type.

Supplemental Figure 3. DNA Methylation Levels in *NPR1* and *PR2*.

Supplemental Figure 4. Numbers of Methylcytosines Identified in *elp2* and the Wild Type.

Supplemental Figure 5. The Density of Methylcytosines and Ratio of the Number of Methylcytosines Identified in *elp2* versus the Wild Type.

Supplemental Figure 6. DNA Methylation Status at the *PAD4* Locus Revealed by the Genome-Wide Bisulfite Sequencing.

Supplemental Figure 7. Pathogen-Induced Dynamic Methylation Changes at Specific Methylcytosines in *NPR1* and *PAD4*.

Supplemental Figure 8. Immune Responses in *Arabidopsis* Mutants Deficient in DNA Methylation/Demethylation.

Supplemental Table 1. Primers Used for Bisulfite-Sequencing PCR.

Supplemental Table 2. Rates of Nonconversion and T-to-C Sequencing Errors in the Chloroplast Reference Genome.

Supplemental Table 3. Primers Used for Real-Time qPCR Analysis.

Supplemental Table 4. Primers Used for ChIP Real-Time qPCR Analysis.

Supplemental Table 5. Results of the Sequence Clean Process.

ACKNOWLEDGMENTS

We thank Robert Fischer (University of California, Berkeley, CA) for *rdd* seeds and the Arabidopsis Biological Resource Center (Ohio State University, Columbus, OH) for *met1-3* and *ddc* seeds. This work was supported by a grant from the National Science Foundation (IOS-0842716) awarded to Z.M. We thank Jin Yao for help with microarray data analysis and Christopher DeFraia for critical comments on the article.

AUTHOR CONTRIBUTIONS

Z.M. conceived and designed the experiments. Y.W., C.A., X.Z., Y.Z., and D.M.A. performed the experiments. J.Y., Y.S., F.Y., and Z.M. analyzed the data. Z.M. wrote the article.

Received January 2, 2013; revised January 29, 2013; accepted February 4, 2013; published February 22, 2013.

REFERENCES

Agorio, A., and Vera, P. (2007). ARGONAUTE4 is required for resistance to *Pseudomonas syringae* in *Arabidopsis*. Plant Cell **19:** 3778–3790.

Aldrich, J., and Cullis, C.A. (1993). CTAB DNA extraction from plant tissues. Plant Mol. Biol. Rep. **11:** 128–141.

Alvarez-Venegas, R., Abdallat, A.A., Guo, M., Alfano, J.R., and Avramova, Z. (2007). Epigenetic control of a transcription factor at the cross section of two antagonistic pathways. Epigenetics **2:** 106–113.

Anderson, S.L., Coli, R., Daly, I.W., Kichula, E.A., Rork, M.J., Volpi, S.A., Ekstein, J., and Rubin, B.Y. (2001). Familial dysautonomia is caused by mutations of the IKAP gene. Am. J. Hum. Genet. **68:** 753–758.

Bauer, F., Matsuyama, A., Candiracci, J., Dieu, M., Scheliga, J., Wolf, D.A., Yoshida, M., and Hermand, D. (2012). Translational control of cell division by elongator. Cell Rep. **1:** 424–433.

Berr, A., Ménard, R., Heitz, T., and Shen, W.H. (2012). Chromatin modification and remodelling: A regulatory landscape for the control of *Arabidopsis* defence responses upon pathogen attack. Cell. Microbiol. **14:** 829–839.

Bormann Chung, C.A., Boyd, V.L., McKernan, K.J., Fu, Y., Monighetti, C., Peckham, H.E., and Barker, M. (2010). Whole methylome analysis by ultra-deep sequencing using two-base encoding. PLoS ONE **5:** e9320.

Cao, H., Glazebrook, J., Clarke, J.D., Volko, S., and Dong, X. (1997). The *Arabidopsis NPR1* gene that controls systemic acquired resistance encodes a novel protein containing ankyrin repeats. Cell **88:** 57–63.

Cao, H., Li, X., and Dong, X. (1998). Generation of broad-spectrum disease resistance by overexpression of an essential regulatory gene in systemic acquired resistance. Proc. Natl. Acad. Sci. USA **95:** 6531–6536.

Century, K.S., Shapiro, A.D., Repetti, P.P., Dahlbeck, D., Holub, E., and Staskawicz, B.J. (1997). *NDR1*, a pathogen-induced component required for *Arabidopsis* disease resistance. Science **278:** 1963–1965.

Chan, S.W., Henderson, I.R., Zhang, X., Shah, G., Chien, J.S., and Jacobsen, S.E. (2006). RNAi, DRD1, and histone methylation actively target developmentally important non-CG DNA methylation in *Arabidopsis*. PLoS Genet. **2:** e83.

Chen, Z., Zhang, H., Jablonowski, D., Zhou, X., Ren, X., Hong, X., Schaffrath, R., Zhu, J.K., and Gong, Z. (2006). Mutations in ABO1/ELO2, a subunit of holo-Elongator, increase abscisic acid sensitivity and drought tolerance in *Arabidopsis thaliana*. Mol. Cell. Biol. **26:** 6902–6912.

Chinenov, Y. (2002). A second catalytic domain in the Elp3 histone acetyltransferases: A candidate for histone demethylase activity? Trends Biochem. Sci. **27:** 115–117.

Choi, S.M., Song, H.R., Han, S.K., Han, M., Kim, C.Y., Park, J., Lee, Y.H., Jeon, J.S., Noh, Y.S., and Noh, B. (2012). HDA19 is required

for the repression of salicylic acid biosynthesis and salicylic acid-mediated defense responses in *Arabidopsis*. Plant J. **71:** 135–146.

Close, P., Hawkes, N., Cornez, I., Creppe, C., Lambert, C.A., Rogister, B., Siebenlist, U., Merville, M.P., Slaugenhaupt, S.A., Bours, V., Svejstrup, J.Q., and Chariot, A. (2006). Transcription impairment and cell migration defects in elongator-depleted cells: Implication for familial dysautonomia. Mol. Cell **22:** 521–531.

Conrath, U. (2011). Molecular aspects of defence priming. Trends Plant Sci. **16:** 524–531.

Creppe, C., et al. (2009). Elongator controls the migration and differentiation of cortical neurons through acetylation of α-tubulin. Cell **136:** 551–564.

DeFraia, C.T., Zhang, X., and Mou, Z. (2010). Elongator subunit 2 is an accelerator of immune responses in *Arabidopsis thaliana*. Plant J. **64:** 511–523.

Dowen, R.H., Pelizzola, M., Schmitz, R.J., Lister, R., Dowen, J.M., Nery, J.R., Dixon, J.E., and Ecker, J.R. (2012). Widespread dynamic DNA methylation in response to biotic stress. Proc. Natl. Acad. Sci. USA **109:** E2183–E2191.

Falk, A., Feys, B.J., Frost, L.N., Jones, J.D.G., Daniels, M.J., and Parker, J.E. (1999). *EDS1*, an essential component of *R* gene-mediated disease resistance in *Arabidopsis* has homology to eukaryotic lipases. Proc. Natl. Acad. Sci. USA **96:** 3292–3297.

Glazebrook, J., Rogers, E.E., and Ausubel, F.M. (1996). Isolation of *Arabidopsis* mutants with enhanced disease susceptibility by direct screening. Genetics **143:** 973–982.

Gruntman, E., Qi, Y., Slotkin, R.K., Roeder, T., Martienssen, R.A., and Sachidanandam, R. (2008). Kismeth: Analyzer of plant methylation states through bisulfite sequencing. BMC Bioinformatics **9:** 371.

Hawkes, N.A., Otero, G., Winkler, G.S., Marshall, N., Dahmus, M.E., Krappmann, D., Scheidereit, C., Thomas, C.L., Schiavo, G., Erdjument-Bromage, H., Tempst, P., and Svejstrup, J.Q. (2002). Purification and characterization of the human elongator complex. J. Biol. Chem. **277:** 3047–3052.

He, X.J., Chen, T., and Zhu, J.K. (2011). Regulation and function of DNA methylation in plants and animals. Cell Res. **21:** 442–465.

Huang, B., Johansson, M.J., and Byström, A.S. (2005). An early step in wobble uridine tRNA modification requires the Elongator complex. RNA **11:** 424–436.

Jablonowski, D., Frohloff, F., Fichtner, L., Stark, M.J., and Schaffrath, R. (2001). *Kluyveromyces lactis* zymocin mode of action is linked to RNA polymerase II function via Elongator. Mol. Microbiol. **42:** 1095–1105.

Jaskiewicz, M., Conrath, U., and Peterhänsel, C. (2011). Chromatin modification acts as a memory for systemic acquired resistance in the plant stress response. EMBO Rep. **12:** 50–55.

Jirage, D., Tootle, T.L., Reuber, T.L., Frost, L.N., Feys, B.J., Parker, J.E., Ausubel, F.M., and Glazebrook, J. (1999). *Arabidopsis thaliana PAD4* encodes a lipase-like gene that is important for salicylic acid signaling. Proc. Natl. Acad. Sci. USA **96:** 13583–13588.

Jones, J.D., and Dangl, J.L. (2006). The plant immune system. Nature **444:** 323–329.

Kim, J.H., Lane, W.S., and Reinberg, D. (2002). Human Elongator facilitates RNA polymerase II transcription through chromatin. Proc. Natl. Acad. Sci. USA **99:** 1241–1246.

Kim, K.C., Lai, Z., Fan, B., and Chen, Z. (2008). *Arabidopsis* WRKY38 and WRKY62 transcription factors interact with histone deacetylase 19 in basal defense. Plant Cell **20:** 2357–2371.

Kinkema, M., Fan, W., and Dong, X. (2000). Nuclear localization of NPR1 is required for activation of *PR* gene expression. Plant Cell **12:** 2339–2350.

Krogan, N.J., and Greenblatt, J.F. (2001). Characterization of a six-subunit holo-elongator complex required for the regulated expression of a group of genes in *Saccharomyces cerevisiae*. Mol. Cell. Biol. **21:** 8203–8212.

Law, J.A., and Jacobsen, S.E. (2010). Establishing, maintaining and modifying DNA methylation patterns in plants and animals. Nat. Rev. Genet. **11:** 204–220.

Li, B., Carey, M., and Workman, J.L. (2007). The role of chromatin during transcription. Cell **128:** 707–719.

Li, J., Brader, G., Kariola, T., and Palva, E.T. (2006). WRKY70 modulates the selection of signaling pathways in plant defense. Plant J. **46:** 477–491.

Lister, R., O'Malley, R.C., Tonti-Filippini, J., Gregory, B.D., Berry, C.C., Millar, A.H., and Ecker, J.R. (2008). Highly integrated single-base resolution maps of the epigenome in *Arabidopsis*. Cell **133:** 523–536.

Liu, X., Yu, C.W., Duan, J., Luo, M., Wang, K., Tian, G., Cui, Y., and Wu, K. (2012). HDA6 directly interacts with DNA methyltransferase MET1 and maintains transposable element silencing in *Arabidopsis*. Plant Physiol. **158:** 119–129.

López, A., Ramírez, V., García-Andrade, J., Flors, V., and Vera, P. (2011). The RNA silencing enzyme RNA polymerase v is required for plant immunity. PLoS Genet. **7:** e1002434.

Lucarelli, M., Fuso, A., Strom, R., and Scarpa, S. (2001). The dynamics of myogenin site-specific demethylation is strongly correlated with its expression and with muscle differentiation. J. Biol. Chem. **276:** 7500–7506.

Luna, E., Bruce, T.J., Roberts, M.R., Flors, V., and Ton, J. (2012). Next-generation systemic acquired resistance. Plant Physiol. **158:** 844–853.

Métivier, R., et al. (2008). Cyclical DNA methylation of a transcriptionally active promoter. Nature **452:** 45–50.

Mishina, T.E., and Zeier, J. (2006). The *Arabidopsis* flavin-dependent monooxygenase FMO1 is an essential component of biologically induced systemic acquired resistance. Plant Physiol. **141:** 1666–1675.

Mosher, R.A., Durrant, W.E., Wang, D., Song, J., and Dong, X. (2006). A comprehensive structure-function analysis of *Arabidopsis* SNI1 defines essential regions and transcriptional repressor activity. Plant Cell **18:** 1750–1765.

Nawrath, C., Heck, S., Parinthawong, N., and Métraux, J.-P. (2002). EDS5, an essential component of salicylic acid-dependent signaling for disease resistance in *Arabidopsis*, is a member of the MATE transporter family. Plant Cell **14:** 275–286.

Nelissen, H., et al. (2010). Plant Elongator regulates auxin-related genes during RNA polymerase II transcription elongation. Proc. Natl. Acad. Sci. USA **107:** 1678–1683.

Nelissen, H., Fleury, D., Bruno, L., Robles, P., De Veylder, L., Traas, J., Micol, J.L., Van Montagu, M., Inzé, D., and Van Lijsebettens, M. (2005). The elongata mutants identify a functional Elongator complex in plants with a role in cell proliferation during organ growth. Proc. Natl. Acad. Sci. USA **102:** 7754–7759.

Nugent, R.L., Johnsson, A., Fleharty, B., Gogol, M., Xue-Franzén, Y., Seidel, C., Wright, A.P., and Forsburg, S.L. (2010). Expression profiling of *S. pombe* acetyltransferase mutants identifies redundant pathways of gene regulation. BMC Genomics **11:** 59.

Okada, Y., Yamagata, K., Hong, K., Wakayama, T., and Zhang, Y. (2010). A role for the elongator complex in zygotic paternal genome demethylation. Nature **463:** 554–558.

Otero, G., Fellows, J., Li, Y., de Bizemont, T., Dirac, A.M., Gustafsson, C.M., Erdjument-Bromage, H., Tempst, P., and Svejstrup, J.Q. (1999). Elongator, a multisubunit component of

a novel RNA polymerase II holoenzyme for transcriptional elongation. Mol. Cell **3:** 109–118.

Otto, C., Stadler, P.F., and Hoffmann, S. (2012). Fast and sensitive mapping of bisulfite-treated sequencing data. Bioinformatics **28:** 1698–1704.

Palma, K., Thorgrimsen, S., Malinovsky, F.G., Fiil, B.K., Nielsen, H.B., Brodersen, P., Hofius, D., Petersen, M., and Mundy, J. (2010). Autoimmunity in *Arabidopsis acd11* is mediated by epigenetic regulation of an immune receptor. PLoS Pathog. **6:** e1001137.

Paraskevopoulou, C., Fairhurst, S.A., Lowe, D.J., Brick, P., and Onesti, S. (2006). The Elongator subunit Elp3 contains a Fe4S4 cluster and binds S-adenosylmethionine. Mol. Microbiol. **59:** 795–806.

Pavet, V., Quintero, C., Cecchini, N.M., Rosa, A.L., and Alvarez, M.E. (2006). *Arabidopsis* displays centromeric DNA hypomethylation and cytological alterations of heterochromatin upon attack by *Pseudomonas syringae*. Mol. Plant Microbe Interact. **19:** 577–587.

Penterman, J., Uzawa, R., and Fischer, R.L. (2007a). Genetic interactions between DNA demethylation and methylation in *Arabidopsis*. Plant Physiol. **145:** 1549–1557.

Penterman, J., Zilberman, D., Huh, J.H., Ballinger, T., Henikoff, S., and Fischer, R.L. (2007b). DNA demethylation in the *Arabidopsis* genome. Proc. Natl. Acad. Sci. USA **104:** 6752–6757.

Rahl, P.B., Chen, C.Z., and Collins, R.N. (2005). Elp1p, the yeast homolog of the FD disease syndrome protein, negatively regulates exocytosis independently of transcriptional elongation. Mol. Cell **17:** 841–853.

Ritchie, M.E., Silver, J., Oshlack, A., Holmes, M., Diyagama, D., Holloway, A., and Smyth, G.K. (2007). A comparison of background correction methods for two-colour microarrays. Bioinformatics **23:** 2700–2707.

Ryals, J., Weymann, K., Lawton, K., Friedrich, L., Ellis, D., Steiner, H.-Y., Johnson, J., Delaney, T.P., Jesse, T., Vos, P., and Uknes, S. (1997). The *Arabidopsis NIM1* protein shows homology to the mammalian transcription factor inhibitor I κ B. Plant Cell **9:** 425–439.

Saleh, A., Alvarez-Venegas, R., and Avramova, Z. (2008). An efficient chromatin immunoprecipitation (ChIP) protocol for studying histone modifications in *Arabidopsis* plants. Nat. Protoc. **3:** 1018–1025.

Saze, H., Mittelsten Scheid, O., and Paszkowski, J. (2003). Maintenance of CpG methylation is essential for epigenetic inheritance during plant gametogenesis. Nat. Genet. **34:** 65–69.

Shah, J., Tsui, F., and Klessig, D.F. (1997). Characterization of a salicylic acid-insensitive mutant (*sai1*) of *Arabidopsis thaliana*, identified in a selective screen utilizing the SA-inducible expression of the *tms2* gene. Mol. Plant Microbe Interact. **10:** 69–78.

Slaugenhaupt, S.A., et al. (2001). Tissue-specific expression of a splicing mutation in the *IKBKAP* gene causes familial dysautonomia. Am. J. Hum. Genet. **68:** 598–605.

Smyth, G.K. (2005). Limma: Linear models for microarray data. In Bioinformatics and Computational Biology Solutions Using R and Bioconductor, R. Gentleman, V. Carey, S. Dudoit, R. Irizarry, and W. Huber, eds (New York: Springer), pp. 397–420.

Song, J.T., Lu, H., and Greenberg, J.T. (2004). Divergent roles in *Arabidopsis thaliana* development and defense of two homologous genes, *aberrant growth and death2* and *AGD2-LIKE DEFENSE RESPONSE PROTEIN1*, encoding novel aminotransferases. Plant Cell **16:** 353–366.

Svejstrup, J.Q. (2007). Elongator complex: How many roles does it play? Curr. Opin. Cell Biol. **19:** 331–336.

Tao, Y., Xie, Z., Chen, W., Glazebrook, J., Chang, H.S., Han, B., Zhu, T., Zou, G., and Katagiri, F. (2003). Quantitative nature of *Arabidopsis* responses during compatible and incompatible interactions with the bacterial pathogen *Pseudomonas syringae*. Plant Cell **15:** 317–330.

Tian, L., Fong, M.P., Wang, J.J., Wei, N.E., Jiang, H., Doerge, R.W., and Chen, Z.J. (2005). Reversible histone acetylation and deacetylation mediate genome-wide, promoter-dependent and locus-specific changes in gene expression during plant development. Genetics **169:** 337–345.

To, T.K., et al. (2011). *Arabidopsis* HDA6 regulates locus-directed heterochromatin silencing in cooperation with MET1. PLoS Genet. **7:** e1002055.

van Wees, S.C.M., de Swart, E.A.M., van Pelt, J.A., van Loon, L.C., and Pieterse, C.M.J. (2000). Enhancement of induced disease resistance by simultaneous activation of salicylate- and jasmonate-dependent defense pathways in *Arabidopsis thaliana*. Proc. Natl. Acad. Sci. USA **97:** 8711–8716.

Versées, W., De Groeve, S., and Van Lijsebettens, M. (2010). Elongator, a conserved multitasking complex? Mol. Microbiol. **76:** 1065–1069.

Wang, C., Gao, F., Wu, J., Dai, J., Wei, C., and Li, Y. (2010). *Arabidopsis* putative deacetylase AtSRT2 regulates basal defense by suppressing *PAD4*, *EDS5* and *SID2* expression. Plant Cell Physiol. **51:** 1291–1299.

Wang, D., Weaver, N.D., Kesarwani, M., and Dong, X. (2005). Induction of protein secretory pathway is required for systemic acquired resistance. Science **308:** 1036–1040.

Wang, L., Mitra, R.M., Hasselmann, K.D., Sato, M., Lenarz-Wyatt, L., Cohen, J.D., Katagiri, F., and Glazebrook, J. (2008). The genetic network controlling the *Arabidopsis* transcriptional response to *Pseudomonas syringae* pv. *maculicola*: Roles of major regulators and the phytotoxin coronatine. Mol. Plant Microbe Interact. **21:** 1408–1420.

Wildermuth, M.C., Dewdney, J., Wu, G., and Ausubel, F.M. (2001). Isochorismate synthase is required to synthesize salicylic acid for plant defence. Nature **414:** 562–565.

Winkler, G.S., Kristjuhan, A., Erdjument-Bromage, H., Tempst, P., and Svejstrup, J.Q. (2002). Elongator is a histone H3 and H4 acetyltransferase important for normal histone acetylation levels in vivo. Proc. Natl. Acad. Sci. USA **99:** 3517–3522.

Wittschieben, B.O., Otero, G., de Bizemont, T., Fellows, J., Erdjument-Bromage, H., Ohba, R., Li, Y., Allis, C.D., Tempst, P., and Svejstrup, J.Q. (1999). A novel histone acetyltransferase is an integral subunit of elongating RNA polymerase II holoenzyme. Mol. Cell **4:** 123–128.

Workman, J.L., and Kingston, R.E. (1998). Alteration of nucleosome structure as a mechanism of transcriptional regulation. Annu. Rev. Biochem. **67:** 545–579.

Xu, D., Huang, W., Li, Y., Wang, H., Huang, H., and Cui, X. (2012). Elongator complex is critical for cell cycle progression and leaf patterning in *Arabidopsis*. Plant J. **69:** 792–808.

Zhou, X., Hua, D., Chen, Z., Zhou, Z., and Gong, Z. (2009). Elongator mediates ABA responses, oxidative stress resistance and anthocyanin biosynthesis in *Arabidopsis*. Plant J. **60:** 79–90.